IEEE Access
Multidisciplinary ⋮ Rapid Review ⋮ Open Access Journal

Received 29 December 2022, accepted 11 January 2023, date of publication 19 January 2023, date of current version 25 January 2023.

Digital Object Identifier 10.1109/ACCESS.2023.3238070

APPLIED RESEARCH

Micro Resistance Spot Welding Optimization for Ultra-Thin Mo-Re Sheet Used in TWT

JIAN WANG, (Member, IEEE), AND FEN LI
Aerospace Information Research Institute, Chinese Academy of Sciences, Beijing 100094, China
Corresponding author: Jian Wang (wjnust@163.com)

This work was supported in part by the Key Deployment Program of Aerospace Information Research Institute, Chinese Academy of Sciences, under Grant 2021000558.

ABSTRACT 30 μm ultra-thin Mo-Re sheet had been joined by micro resistance spot welding (MRSW) and successfully applied to the low heating power cathode of traveling wave tube (TWT). The effects of different welding parameters, surface state and protection conditions on the joint's appearance, micro-structure and lap shear strength (LSS) were analyzed in this paper. The results showed that a 63.5 N LSS of the MRSW joint was obtained under the following conditions: electrode force $F = 9.0$ N, welding current $I = 1000$A, ramping time $t_1 = 5$ms, welding time $t_2 = 2$ms and dip in the alcohol for protection. The fracture occurs in the heat affected zone (HAZ). Using metallurgical microscopy observed the nugget, metallurgical fusion could be found, the diameter of nugget was about Φ0.3 mm, without gas pores. Scanning electron microscopy (SEM) was used to observe the fracture surface. It could be found some ''whisker'' shape diverged from the joint center to the surroundings in HAZ. The electrode tip was observed by energy dispersive spectroscopy (EDS) and optical profiler. It was found that the tip was uneven and adhered the base metal obviously after spark. Additional work about electrode sticking will be required. The thermal test data showed that the use of ultra-thin Mo-Re sheet can reduce a space TWT cathode heating power (CHP) by 0.57 W, which will effectively save satellite energy and improve the expected working life of vacuum electronic devices.

INDEX TERMS Ultra-thin Mo-Re sheet, micro resistance spot welding (MRSW), welding parameters optimization, lap shear strength (LSS), cathode heating power (CHP), traveling wave tube (TWT).

I. INTRODUCTION

Molybdenum rhenium (Mo-Re) alloy has excellent high-temperature mechanical properties, high recrystallization temperature and resistivity for chemical corrosion, commonly used as vacuum electronic devices (VEDs) cathode supporting materials [1], superconducting thin films [2], [3], [4], advanced aero motor propulsion, nuclear fusion reactor [5], [6] and another extreme environment. Many kinds of materials will inevitably be customized with different shapes, connected with themselves or other materials during application. As an efficient and stable connection mode, different welding methods have been proposed and applied to the joint of Mo-Re sheet or wire, such as resistance welding [7], [8], [9], electron beam welding, laser beam welding [10] and vacuum brazing [11], and many reference data have been obtained. The welding difficulties of ultra-thin refractory alloy materials have already been summarized as follows: First, the smaller thickness of the material is, the less thermal inertia of the welding nugget area, which is harmful to the repeated heating of the material or the heating for a long time. It is necessary to accurately control the extremely short power on time. Second, it is difficult to form a sufficient volume nugget at the interface without damaging the outer surface, because refractory alloy has a high melting point, the base metal has small temperature difference between the inner and outer surface. Too small heat input will lead to non-welding, and too large heat input will lead to sticking between the base metal and the electrode [10]. This sticking will lead to tearing of the previous weld nugget, or even tearing of the ultra-thin sheet. Third, molybdenum (Mo) is easy to recrystallize and hot brittle. Although a certain proportion of

The associate editor coordinating the review of this manuscript and approving it for publication was Mauro Gaggero.

rhenium (Re) is added to improve the weldability, excessive heat input will still lead to significant reduction of material strength in the heat affected zone (HAZ). Fourth, the material surface is easy to form oxide film with high melting point. After the first spot is formed, it will have adverse effects on other adjacent and subsequent spots.

In this article, the joining process with 30 μm thickness Mo-47.5Re sheet was carried out. With the increasingly strict requirements of space TWT on cathode heating power (CHP) [13], [14], [15], the thickness of Mo-Re sheet cylinder has also been reduced to 30-50 μm in order to improve thermal resistance and increase thermal insulation performance, while the traditional thickness is about 70-100 μm. When the cathode temperature is 1050°C, thermodynamic analysis and test data showed that the CHP can be reduced about 0.5 W by using 0.03 mm in place of 0.05 mm, and more 0.5 W by using 0.01 mm in place of 0.03 mm. The mechanical strength of all these thicknesses is sufficient, but insufficient welding nugget strength will lead to changes in the relative positions of the cathode and the focusing electrode (FE), affect the stability of the electronic optical system (EOS), and even cause a short circuit between the cathode and the FE.

Micro resistance spot welding (MRSW) is one of the most commonly used methods in the manufacturing process for joining sheet metal together [16], [17], but reports of ultra-thin Mo-Re sheet are very rare. Further research is needed. Considering these difficulties from structural design and material characteristics, referring to the welding specifications of slightly thicker Mo-Re sheet, aluminum alloy, magnesium alloy, etc. [18], [19], [20], it is necessary to adopt high current, short time and low pressure, which is called hard specifications, for spot welding of ultra-thin Mo-Re sheet. The functions of the above three parameters are as follows: large current makes small resistivity generate enough heat, short time to prevent material grain coarsening caused by long time heating, low pressure keeps the contact resistance in a large range.

In this study, an ultra-thin Mo-47.5Re sheet MRSW method design is given in Section II. Section III shows the optimization process of MRSW parameters, and the nugget characteristics obtained by different parameters are analyzed. The MRSW reliability is verified by TWT electron gun vibration test and micro deformation measurement in Section IV, some follow-up research plans also listed in this Section. Finally, the last Section is the summary of the full text.

II. MRSW METHOD DESIGN

The experimental equipment adopts UNITEK DC25 MRSW machine (Energy storage welding machine, the welding time control accuracy is 0.01ms, the maximum welding current is 4000A), UNITEK THIN-LINE 80&88 pneumatic welding head (the welding pressure control range is 2.2-89N), and double self-made tungsten electrodes. The diameter of the negative electrode supported at the bottom is larger, and it is placed horizontally. For each spot welding, rotate a certain angle according to the direction marked in the Figure 1 for

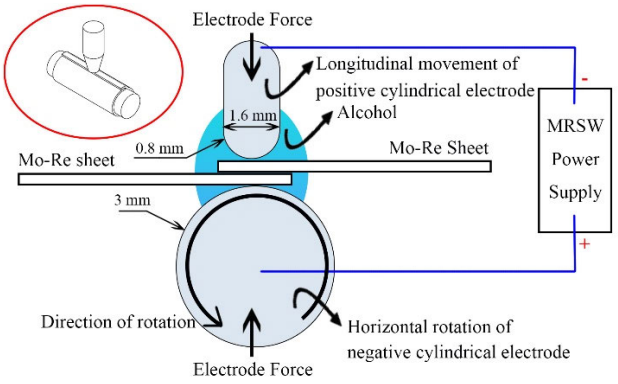

FIGURE 1. Schematic of the welding schedule.

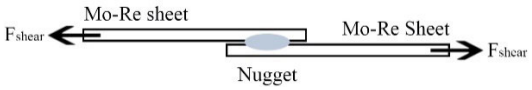

FIGURE 2. Schematic of LSS test.

avoiding too much sticking occur in the near area. Two layers of Mo-47.5Re sheet are stacked on it. The positive electrode rises and falls with the welding head in the vertical direction. The effects of different parameters and surface conditions on the appearance of the spot weld, the microstructure of the joint and the lap shear strength (LSS) properties were analyzed through comparative tests. Determined according to DIN 53283, the LSS is then measured with a tensile machine at a pull rate of 1 mm/min and expressed in MPa on an average of five specimens [21]. The design of the test samples was shown in Figure 2. The microcomputer controlled mechanical testing machine REGER RGM-4200 is used to LSS test. The tension sensor is CELREON STC-50kg.

At the beginning of the experiment, cut the Mo-Re sheet into small squares from the whole sheet. Then, immerse them in acetone solution to remove oil by ultrasonic wave for 30 minutes, and remove the surface oxide film in hydrogen furnace. The heat treatment process parameter is 600 °C hold for 10 min. The contact surfaces of two sheet shall be polished with a rasp or 240 # sandpaper to increase the contact resistance.

The mass fraction of each element of Mo-47.5Re is shown in Table 1. The main physical properties of Mo-47.5Re and other common metal materials are shown in Table 2. ''MRSW solderability W=100*ρ/(λT)'' in the table is still an empirical formula, which aims to explain that Mo-47.5Re material has a not too bad weldability. The ultra-thin structure and high melting point are the direct difficulties facing at present. The welding method designed later will mainly solve these problems. The default welding parameters are shown in Table 3.

III. MRSW PARAMETERS OPTIMIZATION AND DISCUSS

The current, voltage, resistance and power curves obtained by the default parameters are shown in Figure 2.

According to the current curve, the ramp time only spent 3-5 ms, and the target value can be reached within the ramp

TABLE 1. Chemical composition of Mo-47.5Re alloy % (mass).

Major	Impurity content, less than									
Mo	Re	Al	Ga	Fe	Mg	Ni	Si	C	N	O
allowance	47.5	0.002	0.002	0.002	0.001	0.002	0.002	0.005	0.001	0.005

TABLE 2. The major physical properties of Mo-47.5Re and other common metal materials (20°).

Material type	Electrical Resistivity ρ / μΩ·cm	Thermal Conductivity λ / W·cm^{-1}·K^{-1}	Specific heat capacity c / J·g^{-1}·k^{-1}	Coefficient of thermal expansion CTE / μm/m-°C	Melting Point T / °C	MRSW solderability W=100*ρ/(λT)
Mo-47.5Re	22	0.368	0.22	5.72	2450	2.44
Molybdenum (Mo1)	5.6	1.7	0.25	5.2	2895	0.11
Tungsten (WC20)	5.32	1.73	0.16	4.5	3400	0.09
Oxygen-Free Copper (Tu1)	1.75	4.01	0.38	17.5	1356	0.03
Aluminum Alloy (2A12)	7.3	2.37	0.9	22.7	906	0.34
Magnesium Alloy (MA2-1)	12	0.96	1.04	26.0	905	1.38
Tantalum (Ta1)	15.5	0.5447	0.1425	6.5	2996	0.95
Kovar (4J33)	78	0.176	0.502	6.1	1430	30.99

TABLE 3. The default mrsw parameters.

Squeeze time t /ms	Ramp time t /ms	Weld time t /ms	Hold time t /ms	Weld current I /A	Top electrode (-)	Bottom electrode (+)	Electrode Force F / N	Protection conditions
150	5	2	999	1000	WC20	WC20	9.0	Dip in alcohol

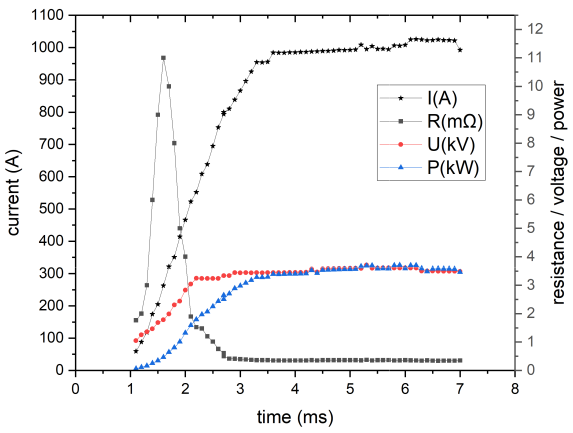

FIGURE 3. The curves obtained by the default parameters.

time. The climbing track of the output current is consistent with the preset curve, indicating that the output capacity of the welding machine meets the welding requirements of large current and short time.

With the increase of current on time, the base metal temperature increases, and the resistivity increases. For example, when the temperature of the base metal rises to 1400 °C, the electrical resistivity of Mo-Re is 84.0 $\mu\Omega$·cm, increase by 3 times of the normal temperature state. The resistance curve shows a steep rise trend in the early stage. When the temperature rises to the softening temperature of Mo-Re, under the pressure of the electrodes, the junction area expands rapidly and the resistance decreases rapidly. When the temperature of the material increases further, metallurgical nuggets begin to appear at the interface, and the resistance decreases further. With the growth of nugget, the conductive area increases and the resistance keeps decreasing. When the nugget cross-section is equivalent to the diameter of electrode tip, it will stop growing, and the resistance will drop to a relatively stable range, which will not continue to decline with the extension of power on time. Based on the above theories and physical phenomena, optimize the MRSW parameters one by one.

A. EFFECT OF MRSW MAIN PARAMETERS

Based on the default parameters in Table 3, first study the effect of different welding currents on the LSS. The results are shown in Figure 4 (a). It can be seen from the figure that the LSS reaches the maximum (68.5 N) at 1100A. When the welding current is greater than 1100A, sticking was very easy to occur, as shown in Figure 4 (b). The electrode and the base metal are severely sticking, some formed weld nuggets would be torn, leaving a hole between the two layers of base metal, and the LSS also decreases significantly. In order to improve the welding stability and electrodes life, we continue to use 1000A for the next test. The LSS (63.5 N, 92.7% of the

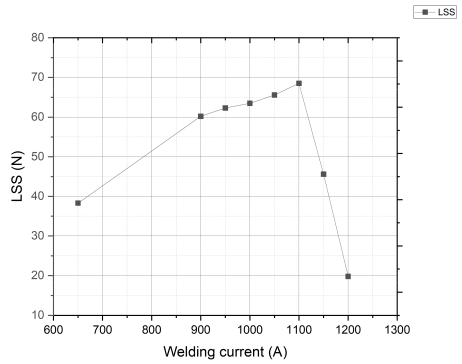

(a) welding current with LSS

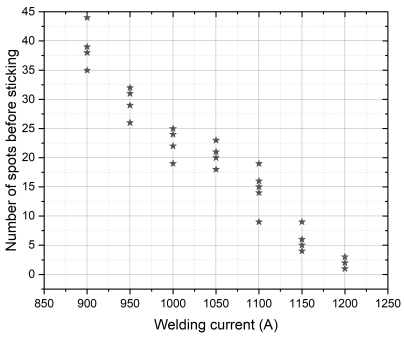

(b) welding current and number of spots before sticking (when the welding current is 600A, there is no sticking occur after 100 times of welding, and the test under 600A is not continued)

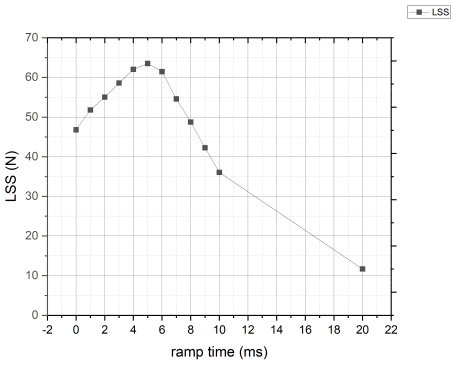

(c) ramp time with LSS

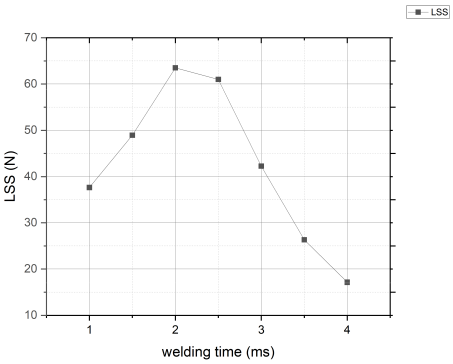

(d) welding time with LSS

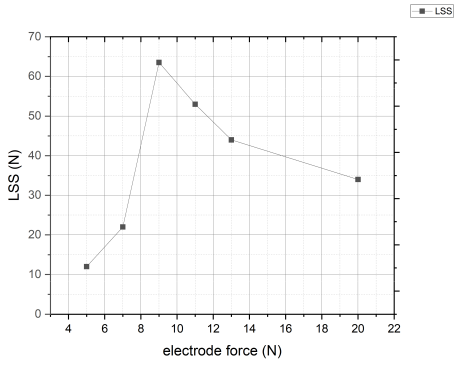

(e) electrode force with LSS

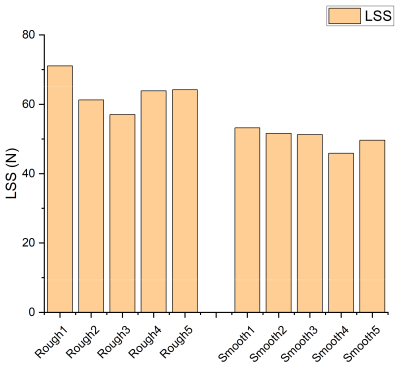

(f) influence of surface roughness

FIGURE 4. Effect of welding parameters.

maximum) obtained under this condition has little difference from the maximum value.

Second, the comparative test results of climbing time are shown in Figure 4 (c). When the climbing time within 5 ms, the longer the ramp time is, the stronger the welding nugget is. However, when the ramp time was set greater than 5 ms, the LSS decreased significantly. Through analysis, it can be considered that with the extension of ramp time, the contact surface softened, the interface resistance decreased significantly, and the large contact resistance at the beginning was not fully utilized to release enough heat, which ultimately leads to insufficient heat to melt the base metal.

Third, the comparative test results of welding time were shown in Figure 4 (d). We found 2ms was the best parameter. When it is less than 2ms, the heat input was insufficient, while more than 2ms, sticking was very easy to occur. Moreover, as shown in Figure 5, the samples after LSS test showed that the fracture occurred in HAZ, the material have defects due to excessive heat input, so the welding current should not be increased.

Last, the comparative test results of electrode force are shown in Figure 4 (e). According to the previous test results, the electrode sticking occurred only after being used dozens of times, which was a sign of insufficient pressure. If the pressure was reduced, sticking would be more likely to

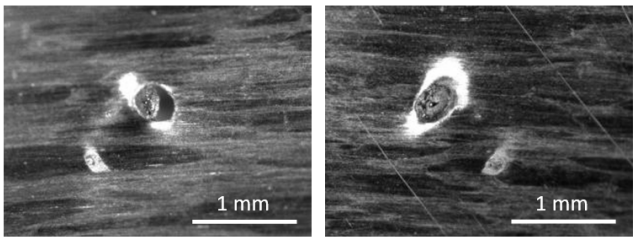

(a) hole (b) adhesion

FIGURE 5. The image of weld nugget after shear.

occur, but after the pressure was increased, although sticking was not easy to occur, LSS had significantly decreased. Therefore, according to the standard of MRSW, the default parameters, proposed in this paper, was an insufficient pressure process specification. These parameters would lead to excessive contact resistance between electrodes and base metal, which will damage the electrode while forming nuggets on the base metal contact surface. Additional work about electrode sticking will be required to extend electrode life.

B. INFLUENCE OF SURFACE STATE

Use TH2513 DC low resistance tester (DCLRT) to test the contact resistance. The pressure of the welding head was set to 9.0 N. When the two electrodes are directly short circuited, the DCLRT was set to zero. Place two clean Mo-Re sheet between the two electrodes, and the resistance was 25.6 mΩ. After polishing the contact surface of two sheet skins with 240 # sandpaper, the resistance become to 40 mΩ. Continue to use the rasp to grind out large scratches, and the resistance changed to 43 mΩ.

It can be seen that the contact resistance of rough surfaces significantly increased. 240 # sandpaper or rasp grinding has no significant difference. According to the heating formula of resistance welding

$$Q = I^2 \cdot R \cdot t \tag{1}$$

the contact area of two layers of Mo-Re sheet will generate more heat. The welding and LSS tests using the default parameters in Table 3 showed that the LSS of the sample without grinding was only 50.3 N, as shown in Figure 4(f), which was 20.8% lower than that of the sample after grinding.

C. CHARACTERIZATION MICROSTRUCTURE ANALYSIS

The formula for making metallographic corrosion solution is: 5% potassium ferricyanide (K3[Fe(CN)6]) solution and 10% sodium hydroxide (NaOH) solution, which should be prepared separately, mixed when using, cleaned and dried after wiping for 3-5 seconds. Observe the nugget obtained with welding current of 600A, 1000A and 1200A by an upright metallographic microscope Nikon ECLIPSE LV100. As shown in Figure 6. The nugget corresponding to 600A still has the original interface between two layers of base metal. Metallurgical fusion exists in the weld nugget corresponding to 1000A, and the diameter of the weld nugget is about Φ 0.3 mm, the nugget height runs through two layers of base metal, and there are no gas pores in the nugget. While in [22] and [23], gas pores are inevitable.

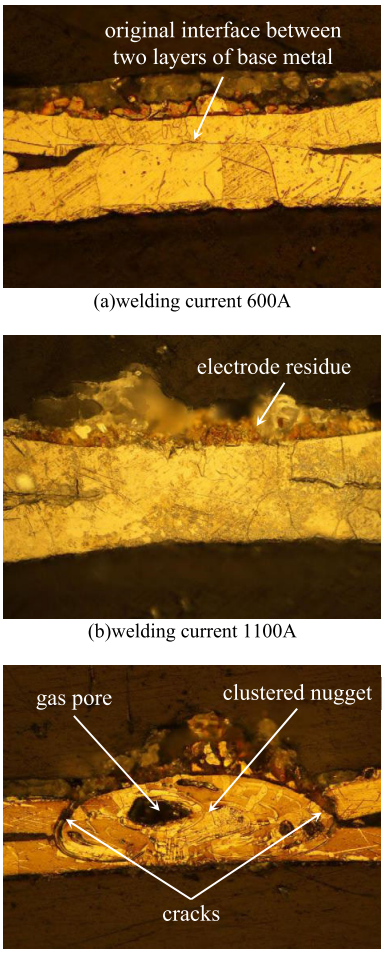

(a)welding current 600A

(b)welding current 1100A

(c) welding current 1200A

FIGURE 6. The metallurgical micro-morphology of weld nugget.

The shear strength σ_c of the welding nugget is

$$\sigma_c = \frac{F}{S} = \frac{63.5}{\pi(\frac{0.3}{2})^2} = 894.37MPa \tag{2}$$

reached 75.8% of the base metal tensile strength (1180 MPa). [10] reported by using electron beam welding, an Mo-44.5 wt%Re alloy was welded successfully, with the welds having an ultimate strength of 821.8-885.3 MPa, similar to the results in this paper. The strength of the weld was enhanced from 100.0 N to 113.0 N in [22], no more than 2 times of this paper (63.5N), while the thickness of the test specimen in [22] is 0.127 mm, 4 times of this paper (0.03 mm).

Because the original grain size is equivalent to the thickness of the base metal, it is difficult to evaluate whether the grains in the nugget grow up. There is obvious electrode residue on the side near the upper electrode. The nugget

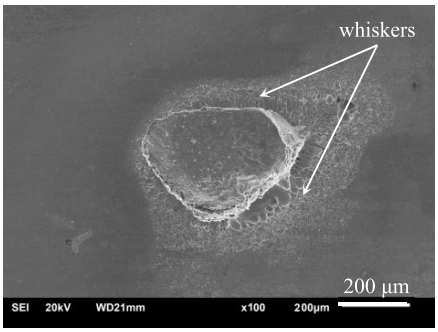

FIGURE 7. The scanning electron micrograph of weld nugget after tear.

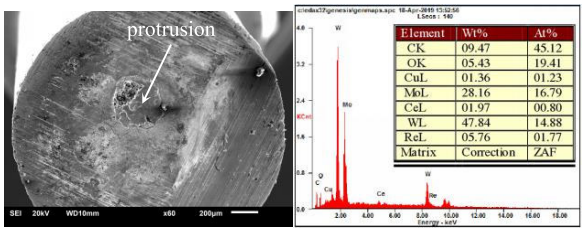

FIGURE 8. The EDS analysis of electrode tip.

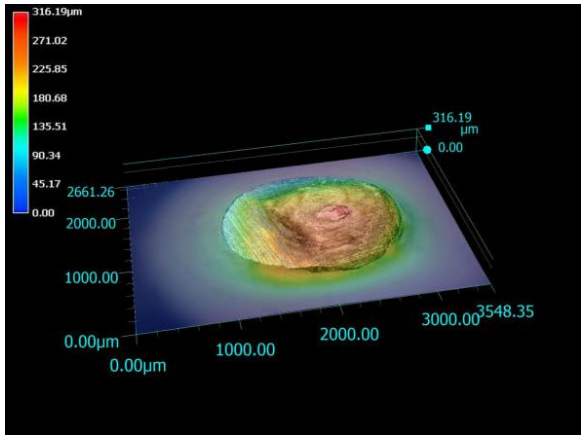

FIGURE 9. The image of electrode tip after spark.

corresponding to 1200A has severe recrystallization, and the nugget is clustered, with obvious cracks with the base metal.

JEOL JSM-6510 scanning electron microscope (SEM) was used to detect the torn welding nuggets, and it can be found that the appearance of ''whiskers'' spread around the center of the spot, as shown in Figure 7. Use the energy dispersive X-ray spectrometer (EDS) APOLLO PRIME added to the scanning electron microscope to analyze the metal components adhered to the electrode tip, and the results are shown in Figure 8. Use KEYENCE VHX-5000 optical profiler to conduct 3D imaging analysis the upper electrode tips, and the results are shown in Figure 9.

The mass fraction of Re was more than 5% in WC20 electrodes, which was not originally included. The analysis of surface morphology shows that the height difference of electrode tip reaches 316.19 μm. On the electrode tip, the base metal is adhered, and a new protrusion is formed. The

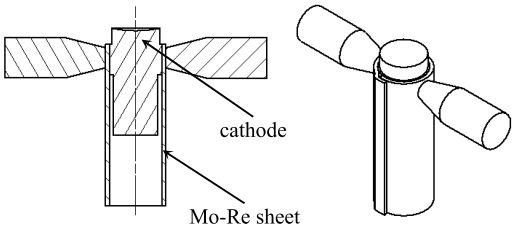

FIGURE 10. Ultra-thin Mo-Re sheet cylinder used for TWT electron gun cathode support.

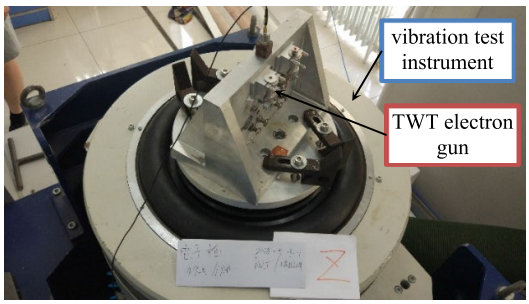

FIGURE 11. TWT electron gun and vibration test instrument.

TABLE 4. Target spectrum table parameters.

Frequency (Hz)	Acceleration ((g)2/Hz)	Left slope (dB/Oct)	Right slope (dB/Oct)
10	0.0502145	/	4
95	1	4	0
130	1	0	-4.84369
200	0.5	-4.84369	0
800	0.5	0	-9.35085
1000	0.25	-9.35085	0
1500	0.25	0	-12
2000	0.0794136	-12	/

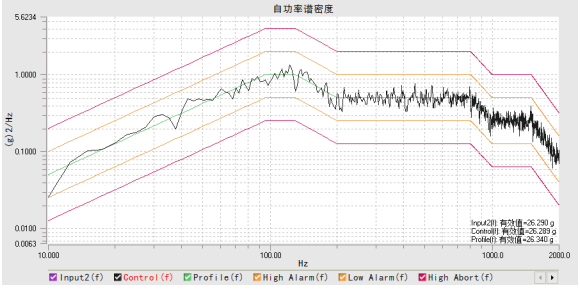

FIGURE 12. Vibration energy spectrum.

protrusion is about Φ0.25 mm, equivalent to the nugget diameter. We believe that this protrusion is growing with each spot, which will lead to the electrode tip becoming more and more irregular, smaller contact area between base metal and electrode, and larger resistance between them. Finally serious sticking will occur, tearing the base metal. Therefore, the use times of an upper electrode should not exceed 15 times.

TABLE 5. Comparison of CHP and maximum change in horizontal direction.

No.	thickness	CHP	X_1 (mm)	Y_1 (mm)	X_2 (mm)	Y_2 (mm)	$\triangle X$ (mm)	$\triangle Y$ (mm)
1-1#	0.03 mm	3.63 W	0.0089	-0.0068	0.0089	-0.0060	0.0000	0.0008
1-2#	0.03 mm	3.39 W	-0.0060	0.0028	-0.0090	0.0027	0.0030	0.0001
1-3#	0.03 mm	3.38 W	0.0035	0.0114	0.0024	0.0071	0.0011	0.0043
1-4#	0.03 mm	3.56 W	-0.0100	-0.0126	-0.0073	-0.0127	0.0027	0.0001
1-5#	0.03 mm	3.46 W	-0.0011	0.0009	-0.0014	0.0009	0.0003	0.0000
Average of CHP (0.03 mm)		**3.48 W**	**Maximum change in horizontal direction before and after vibration (0.03 mm)**				**0.0030**	**0.0043**
2-1#	0.05 mm	4.13 W	0.0034	-0.0034	0.0041	-0.0018	0.0007	0.0016
2-2#	0.05 mm	3.71 W	0.0033	0.0002	0.0048	0.0001	0.0015	0.0001
2-3#	0.05 mm	4.25 W	-0.0051	0.0057	-0.0040	0.0081	0.0011	0.0024
2-4#	0.05 mm	3.92 W	0.0101	-0.0108	0.0063	-0.0138	0.0038	0.0030
2-5#	0.05 mm	4.23 W	-0.0011	0.0009	-0.0010	0.0007	0.0001	0.0002
Average of CHP (0.05 mm)		**4.05 W**	**Maximum change in horizontal direction before and after vibration (0.05 mm)**				**0.0038**	**0.0030**

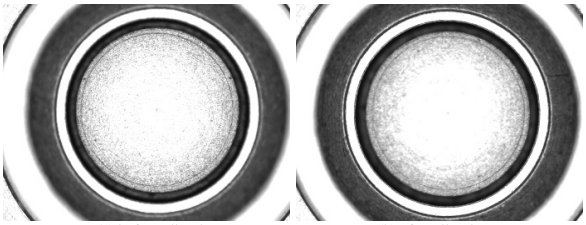

(a) before vibration (b) after vibration

FIGURE 13. No obvious deformation of cathode.

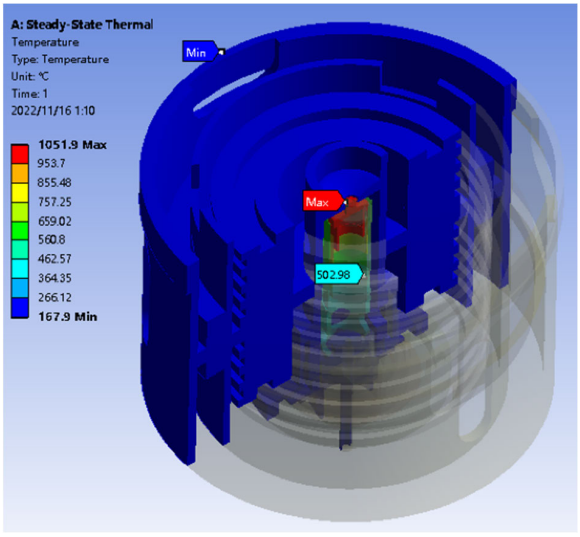

FIGURE 14. ANSYS simulation result of CHP and temperature distribution.

IV. MRSW APPLICATION AND VERIFICATION IN ELECTRON GUN

As shown in Figure 10, the Mo-Re sheet was prepared into a cylinder and welded with the cathode and other supporting structures to complete the fabrication of TWT electron gun. TWT has to face several mechanical vibrations loads during satellite launching and upper stage separation. Therefore, it is important to study the effect of vibration on electron gun [24], [25]. Then, place the electron gun on the vibration test instrument, shown in Figure 11, and set the target spectrum of random vibration to 26.4 grms, lasting for 3 min in axial and radial directions respectively. The target spectrum table parameters were shown in Table 4 and Figure 12. Before and after the vibration, an optical measuring machine (OMM) Nikon VMA2520 was used to detect the maximum change in horizontal direction of the cathode. The test results, as shown in Figure 13 and Table 5, showed the average of CHP reduced 0.57W, close to the ANSYS simulation result in Figure 14, and the deformation of both thicknesses is about 3-4 μm. This showed that the thermodynamics application verification test was passed after changing the material thickness.

V. CONCLUSION

For the MRSW of ultra-thin refractory alloy, a set of parameters was proposed in this paper. Under 1000 A welding current, 5 ms climbing time, 2 ms welding time, 9.0 N electrode force, 150 ms preloading time, 999 ms holding time after welding, and dig in the alcohol, an ideal joint without gas pores was obtained. The average of LSS was 63.5N. The above process parameters have the disadvantage of sacrificing electrode life, because the electrode tip was easy contaminated by the base metal, resulting in reduced contact area and excessive contact resistance, which was the main reason for sticking.

The new technology and new materials had been successfully applied to TWT electron gun, and the CHP had been reduced 0.57 W. In the future, it is still of great significance to continue exploring the rolling and welding of 0.02mm, even 0.01mm Mo-Re sheet. This has been proved to be an effective way to reduce CHP.

ACKNOWLEDGMENT

The authors would like to acknowledge Fei Li for his helpful discussion on the application validation, Cha Gao for providing thermodynamic simulation and test methods, Yongliang Liu, Xinai Liu, and Yu Fan for the selection of test conditions, Rui Guo from the School of Electronic, Electrical and Communication Engineering, UCAS, as well as staff members of the Process Team for their contribution towards this work.

REFERENCES

[1] J. O. Tarter, P. Swartzentruber, J. Balk, A. Fryman, C. Rabek, and A. Batts, "Variations in properties of Mo-Re sheet—Effects on dispenser cathode fabrication," in *Proc. IVESC*, Apr. 2012, pp. 477–478, doi: 10.1109/IVESC.2012.6264203.

[2] A. Shapovalov, O. Boliasova, M. Belogolovskii, and O. Kalenyuk, "Two-band/two-gap superconductivity in molybdenum-rhenium alloys," in *Proc. IEEE 12th Int. Conf. Electron. Inf. Technol. (ELIT)*, May 2021, pp. 242–245, doi: 10.1109/ELIT53502.2021.9501131.

[3] A. Andreone, A. Barone, A. D. Chiara, G. Mascolo, V. Palmieri, G. Peluso, and U. S. di Uccio, "Mo-Re superconducting thin films by single target magnetron sputtering," *IEEE Trans. Magn.*, vol. 25, no. 2, pp. 1972–1975, Mar. 1989, doi: 10.1109/20.92695.

[4] C. Tseng, H. Liu, and C. Lue, "NMR study of electronic properties in Mo7Re13B and W7Re13B superconductors," in *Proc. IEEE Magn. Conf. (INTERMAG)*, May 2015, p. 1, doi: 10.1109/INTMAG.2015.7156958.

[5] X. Qiu, H. Pang, G. Ran, Y. Xin, Y. Li, Q. Han, W. Li, X. Chai, S. Gao, Q. Li, Y. Li, and Y. Jiao, "In-situ TEM observation of loop evolution in MO-5Re alloy under Fe+ irradiation," *J. Nucl. Mater.*, vol. 559, Feb. 2022, Art. no. 153443, doi: 10.1016/j.jnucmat.2021.153443.

[6] F. Morito, V. P. Chakin, M. I. Danylenko, and A. V. Krajnikov, "Radiation-induced strengthening in EB welds of Mo–Re alloys during high temperature neutron irradiation," *J. Nucl. Mater.*, vol. 417, nos. 1–3, pp. 976–979, Oct. 2011, doi: 10.1016/j.jnucmat.2010.12.183.

[7] J. Farrell, W. Umstead, J. Xu, and T. Zhai, "Resistance spot welding of 50Mo-50Re refractory alloy foils," in *Proc. IEEE Int. Vac. Electron. Conf. Jointly IEEE Int. Vac. Electron Sources*, Apr. 2006, pp. 363–364, doi: 10.1109/IVELEC.2006.1666333.

[8] Y. Lu, E. Mayton, H. Song, M. Kimchi, and W. Zhang, "Dissimilar metal joining of aluminum to steel by ultrasonic plus resistance spot welding–microstructure and mechanical properties," *Mater. Design*, vol. 165, Mar. 2019, Art. no. 107585, doi: 10.1016/j.matdes.2019.107585.

[9] Y. Lu, D. D. Sage, C. Fink, and W. Zhang, "Dissimilar metal joining of aluminium to zinc-coated steel by ultrasonic plus resistance spot welding—Microstructure and mechanical properties," *Sci. Technol. Weld. Joining*, vol. 25, no. 3, pp. 217–218, 2020, doi: 10.1080/13621718.2019.1667051.

[10] D. P. Kramer, J. R. McDougal, B. A. Booher, J. D. Ruhkamp, E. I. Howell, and J. J. Kwiatkowski, "Electron beam and Nd-YAG laser welding of niobium-1% zirconium and molybdenum-44.5% rhenium thin select material," in *Proc. Collection Tech. Papers. 35th Intersociety Energy Convers. Eng. Conf. Exhibit*, vol. 2, 2000, pp. 956–961, doi: 10.1109/IECEC.2000.870896.

[11] D. Busbaher and D. P. Sekulic, "Wetting of Mo/Ni nano-composites for dispenser cathode Mo/Re brazing applications," in *Proc. IEEE Int. Vac. Electron. Conf.*, Apr. 2009, pp. 563–564, doi: 10.1109/IVELEC.2009.5193469.

[12] S. J. Dong, G. P. Kelkar, and Y. Zhou, "Electrode sticking during micro-resistance welding of thin metal sheets," *IEEE Trans. Electron. Packag. Manuf.*, vol. 25, no. 4, pp. 355–361, Oct. 2002, doi: 10.1109/TEPM.2002.807732.

[13] W. Jiang, J. Wang, Y. Luo, L. Xu, X. Yao, and S. Wang, "Thermal analysis of sheet beam gun for the sheet beam traveling wave tube," *IEEE Trans. Electron Devices*, vol. 63, no. 3, pp. 1312–1316, Mar. 2016, doi: 10.1109/TED.2016.2519041.

[14] S. Yu, M. Meng, X. Su, H. Fan, and Y. Xin, "An improved low power heater cathode assembly for space-TWT," in *Proc. 8th Int. Vac. Electron Sources Conf. Nanocarbon*, Oct. 2010, pp. 260–261, doi: 10.1109/IVESC.2010.5644266.

[15] H. Wang, W. Shao, and M. Zhang, "Simulation and test of cathode heating power and temperature distribution," in *Proc. IEEE Int. Vac. Electron. Conf.*, Apr. 2014, pp. 527–528, doi: 10.1109/IVEC.2014.6857722.

[16] C. Yuhua, L. Shuhan, L. Dongya, and C. Wenming, "Characteristics and mechanical properties of joints of Ti/Al dissimilar metal by micro resistance spot welding," *Rare Metal Mater. Eng.*, vol. 46, no. S1, pp. 36–40, 2017.

[17] Y.-J. Xia, Z.-W. Su, M. Lou, Y.-B. Li, and B. E. Carlson, "Online precision measurement of weld indentation in resistance spot welding using servo gun," *IEEE Trans. Instrum. Meas.*, vol. 69, no. 7, pp. 4465–4475, Jul. 2020, doi: 10.1109/TIM.2019.2943981.

[18] B. Djokić, "Calibrations of resistance welding equipment with high pulsed currents," *IEEE Trans. Instrum. Meas.*, vol. 64, no. 6, pp. 1767–1772, Jun. 2015, doi: 10.1109/TIM.2015.2399011.

[19] A. Hasanniah and M. Movahedi, "Welding of Al-Mg aluminum alloy to aluminum clad steel sheet using pulsed gas tungsten arc process," *J. Manuf. Processes*, vol. 31, pp. 494–501, Jan. 2018, doi: 10.1016/j.jmapro.2017.12.008.

[20] M. Pouranvari, "Critical assessment 27: Dissimilar resistance spot welding of aluminium/steel: Challenges and opportunities," *Mater. Sci. Technol.*, vol. 33, no. 15, pp. 1705–1712, Oct. 2017, doi: 10.1080/02670836.2017.1334310.

[21] N. Chen, H.-P. Wang, B. E. Carlson, D. R. Sigler, and M. Wang, "Fracture mechanisms of Al/steel resistance spot welds in lap shear test," *J. Mater. Process. Technol.*, vol. 243, pp. 347–354, May 2017, doi: 10.1016/j.jmatprotec.2016.12.015.

[22] J. Xu and T. Zhai, "The small-scale resistance spot welding of refractory alloy 50Mo-50Re thin sheet," *JOM*, vol. 60, no. 7, pp. 80–83, Jul. 2008, doi: 10.1007/s11837-008-0096-x.

[23] P. Liu, K.-Y. Feng, and G.-M. Zhang, "A novel study on laser lap welding of refractory alloy 50Mo–50Re of small-scale thin sheet," *Vacuum*, vol. 136, pp. 10–13, Feb. 2017, doi: 10.1016/j.vacuum.2016.11.001.

[24] C. Mistry and S. K. Ghosh, "Effect of vibration on the cathode lead of electron gun assembly of the travelling wave tube," in *Proc. URSI Regional Conf. Radio Sci. (URSI-RCRS)*, Feb. 2020, pp. 1–2, doi: 10.23919/URSIRCRS49211.2020.9113644.

[25] H. Tian, H. Xu, W. Qi, Y. Liu, and P. Huang, "The reliability simulation of space TWT," in *Proc. IEEE Int. Vac. Electron. Conf. (IVEC)*, Apr. 2015, pp. 1–2, doi: 10.1109/IVEC.2015.7224017.

JIAN WANG (Member, IEEE) was born in Tianjin, in May 1989. He received the B.S. and M.S. degrees from the Nanjing University of Science and Technology (NUST), Nanjing, China, in 2012 and 2015, respectively.

Since 2015, he has been working as an Assistant Researcher with the Research and Development Center for Microwave Devices and Systems, Aerospace Information Research Institute, Chinese Academy of Sciences (AIRCAS, original IECAS), Beijing, China. He involved in the design and development of a series of high quality, high frequency, high power, broadband, and high-efficiency TWT fabrication technology. His research interests include TWT EOS design, digitization, automation and informatization fabrication, precision assembly technology, brazing, laser beam welding (LBW), electron beam welding (EBW), and deformation control technology.

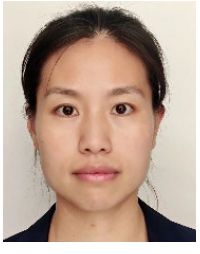

FEN LI received the M.S. degree in material processing engineering from Beihang University, Beijing, China, in 2012. Her work is focused on key technology and structural analysis of TWT. She is currently an Engineer with the Research and Development Center for Microwave Devices and Systems, Aerospace Information Research Institute, Chinese Academy of Sciences (AIRCAS, original IECAS), where she is performing research on functional coatings, including low secondary emission films, and thermal conductivity films.